The Cryosphere
Discussions

Bromine, iodine and sodium in surface snow along the 2013 Talos Dome – GV7 traverse (Northern Victoria Land, East Antarctica)

Niccolò Maffezzoli[1], Andrea Spolaor[2,3], Carlo Barbante[2,3], Michele Bertò[2], Massimo Frezzotti[4], Paul Vallelonga[1]

[1]Centre for Ice and Climate, Niels Bohr Institute, University of Copenhagen, Juliane Maries Vej 30, Copenhagen Ø 2100, Denmark
[2]Ca'Foscari University of Venice, Department of Environmental Science, Informatics and Statistics, Via Torino 155, 30170 Mestre, Venice, Italy
[3]Institute for the Dynamics of Environmental Processes, IDPA-CNR, Via Torino 155, 30170 Mestre, Venice, Italy
[4]ENEA, SP Anguillarese 301, 00123 Rome, Italy

Correspondence to: Niccolò Maffezzoli (maffe@nbi.ku.dk)

Abstract. Halogen chemistry in the polar regions occurs through the release of sea salt rich aerosols from sea ice surfaces and organic compounds from algae colonies living within the sea ice environment. Measurements of halogen species in polar snow samples are limited to a few sites although they are shown to be closely related to sea ice extent. We examine here total bromine, iodine and sodium concentrations in a series of 2 m cores collected during a traverse from Talos Dome (72°48' S, 159°06' E) to GV7 (70°41' S, 158°51' E), analyzed by Inductively Coupled Plasma Sector Field Mass Spectrometry (ICP-SFMS) at a resolution of 5 cm. We find a distinct seasonality of the bromine enrichment signal in all cores, with maxima during the austral late spring. Iodine showed average concentrations of 0.04 ppb with little variability. No distinct seasonality was found for iodine and sodium.
The transect revealed homogeneous fluxes for the three chemical species along the transect, due to competing effects of air masses originating from the Ross Sea and the Southern Ocean. The flux measurements are consistent with the uniform values of BrO and IO detected from satellite observations. Similar trends are found for annual bromine enrichment and 130-190° E First Year Sea Ice for the 2010-2013 period.

Keywords: bromine, iodine, sodium, sea ice, Antarctica, halogens, polar halogen chemistry, Talos Dome.

1. Introduction

Halogen elements play an important role in polar boundary layer chemistry. The release of reactive halogen species from sea ice substrates has been demonstrated to be crucial in the destruction of tropospheric ozone layer at polar latitudes (so called Ozone Depletion Events) during springtime (Barrie et al., 1988).

Although the ocean is the major reservoir of bromine, young sea ice surfaces have high salinity and are therefore a source of bromine halides. Brines, salty aqueous solutions and salty blowing snow on sea ice provide highly efficient saline substrates for reactive halogen activation and release in the atmosphere (Saiz-Lopez et al., 2012).

Bromine radicals result from the photolysis of molecular bromine leading to formation of bromine oxide, BrO, through catalytic reactions that destroy ozone molecules. These chemical cycles have been confirmed by satellite Multi AXis-Differential Optical Absorption Spectroscopy (MAX-DOAS) observations of tropospheric BrO over polar regions (Schönhardt et al., 2012). Bromine can then be recycled and re-emitted from halogen-rich condensed phases (sea salt aerosol) or from sea ice surfaces (Pratt et al., 2013), leading to an exponential increase of bromine in the gas phase (Vogt et al., 1996). Such reactions, known as bromine explosions, also lead to enhanced bromine deposition in surface snowpack. Bromine enrichment in snow (compared to sodium, relative to sea water) has therefore been recently used to reconstruct sea ice variability from ice cores both in the Antarctic and Arctic regions (Spolaor et al., 2013b, 2016).

Iodine is emitted by ocean biological colonies and sea ice algae (Vogt et al., 1999; Atkinson et al., 2012) mainly in the form of organic alkyl iodide (R-I) and possibly other compounds. These can be released by wind forced sea spray generation or percolation up to the sea ice surface through brine channels, and are subsequently photolyzed to inorganic species. Plumes of enhanced IO concentrations from satellites and ground based measurements were observed over Antarctic coasts, suggesting a link with biological and chemical sea ice related processes (Schönhardt et al., 2008; Saiz-Lopez et al., 2007). Yet only sporadic events with IO concentrations above detection limits have been observed in the Arctic regions, possibly due to the greater thickness and lower porosity of Arctic sea ice which prevents an efficient release of iodine species in the atmosphere (Mahajan et al., 2010).

Measurements of sea ice related species such as bromine and iodine could therefore allow a sea ice signature to be obtained from ice core records. Until recently, only sodium has been used to qualitatively reconstruct sea ice at glacial-interglacial timescales (e.g. Wolff et al., 2006), but this proxy has limitations at annual and decadal scales, because of the noise input caused by meteorology and open water sources (Abram et al., 2013). Methane sulfonic acid (MSA) is an end product of the oxidation of dimethylsulfide (DMS), which is produced by phytoplankton. MSA deposition has been successfully linked to Antarctic winter sea ice extent (Curran et al., 2003; Abram et al., 2010) on decadal to centennial scales. Yet, the correlation between MSA records and satellite sea ice observations have been shown to be strongly site dependent (Röthlisberger et al., 2009). Post-depositional processes causing loss and migration in the ice layers have also been widely reported to affect MSA, especially in Greenland and at low accumulation sites (Delmas et al., 2003; Weller et al., 2004; Isaksson et al., 2005; Abram et al., 2008).

Victoria Land has been intensively studied for the past two decades. The Taylor Dome (Grootes et al., 2001) and Talos Dome (Stenni et al., 2011) deep ice cores respectively provide 150 kyr and 300 kyr climatic records directly influenced by marine airmasses. Studies on aeolian mineral dust concentration (Delmonte et al., 2010; 2013, Albani et al.,2012) and elemental composition (Vallelonga et al., 2013, Baccolo et al.,2016) were carried out in Talos Dome to understand dust deposition and provenance to Victoria Land.
Albani et al. (2008) pointed out the presence of marine compounds (ikaite) at Talos Dome, typically formed at the early stages of sea ice formation. Back trajectory calculations show that favourable events for air mass advection from the sea ice surface to Talos Dome are rare but likely to occur.
Within the framework of the ITASE program (International Trans-Antarctic Scientific Expedition, Mayewski et al., 2005), several traverses were carried out to evaluate the spatial patterns of isotopic values and chemical species (Magand et al., 2004; Proposito et al., 2002; Becagli et al., 2004, 2005; Benassai et al., 2005).

We present here bromine, iodine and sodium deposition in coastal East Antarctica, by investigating their total concentrations within a series of shallow firn cores, covering the 2010-2013 time period. The cores

86 were drilled during a traverse performed in late December 2013 in Victoria Land (East Antarctica), from Talos
87 Dome (72°48' S, 159°06' E) to GV7 (70°41' S, 158°51' E). The variability of these species at sub-annual
88 timescales will inform on timing and seasonality as well as spatial patterns of their deposition. Such
89 information is necessary for the interpretation at longer timescales of these elements and possible depositional
90 or post depositional effects. These sub-annual resolution investigations are still limited to the Indian sector
91 (Law Dome - Spolaor et al., 2014) and the Atlantic sector (Neumayer station - Frieß et al., 2010) of Antarctica.
92 This study will test the regional variability of these tracers, providing measurements from the Ross Sea to the
93 Indian sector that remains otherwise unstudied.
94

2. Sampling and analyses

2.1 Traverse sampling

98 The traverse was performed in the northern Victoria Land region of East Antarctica (Fig. 1) from the 20th
99 November 2013 to the 8th January 2014. The starting and ending locations were Talos Dome (72°48'S, 159°12'
100 E) and location '6' (see Fig. 1), close to GV7 (70°41' S, 158°51' E), for a total distance of about 300 kilometers.
101 Talos Dome (275 km WNW from Mario Zucchelli station) is located approximately 250 km from the Ross
102 Sea and 290 km from the Indian Ocean. GV7 is a peripheral site on the ice divide coming from Talos Dome,
103 located just 95 km from the Indian Ocean.

104 During the transect, seven shallow cores, labelled hereafter TD (Talos Dome), 10, 9, GV7, 8, 7 and 6 were
105 hand drilled to 2 -m depth (except for GV7 which was 2.5 m). The main characteristics of the coring sites are
106 reported in Table 1. Density profiles were obtained from each core immediately after drilling.

107 The hand auger had a diameter of 10 cm and consisted of an aluminum barrel equipped with fiberglass
108 extensions. The cores were sampled in the cold laboratory at Cà Foscari University of Venice under a class-
109 100 laminar flow hood. Each core was cut with a commercial hand saw and decontaminated
110 through mechanical chiseling by removing approximately 1 cm of the external layer. Every tool was cleaned
111 repeatedly with Ultrapure water. The cores were then subsampled at 5 cm resolution (3 cm for the GV7 core)
112 into polyethylene vials previously cleaned with UPW and then kept frozen at -20 °C until analysis.

2.2 Analytical measurements

114 Total sodium (Na), bromine (Br) and iodine (I) concentrations were determined by Inductively Coupled Plasma
115 - Sector Field Mass Spectrometry (ICP-SFMS Element2, ThermoFischer, Bremen, Germany) at Cà Foscari
116 University of Venice. For a detailed description of the analytical method, see Spolaor et al., 2013a. Each
117 analytical run was started and ended by a UPW cleaning session of 3 min to ensure a stable background level
118 throughout the analysis.
119

120 The external standards that were used to calibrate the analytes were prepared by diluting a 1000 ppm stock IC
121 solution (TraceCERT® purity grade, Sigma-Aldrich, MO, USA). The standard concentrations ranged between
122 10 and 4000 ppt. The calibration regression lines showed correlation coefficients $R^2 > 0.99$ (N=6, p=0.05). The
123 detection limits, calculated as three times the standard deviation of the blanks, were 50 and 5 ppt for bromine
124 and iodine respectively and 0.8 ppb for sodium.
125 Procedural UPW blanks were analyzed periodically to test the cleanliness of the instrument lines. Precautions
126 were also taken to minimize the exposure of the samples to direct light, in order to minimize bromine and
127 iodine photolysis reactions.
128

129 Stable isotopes of water (^{18}O and D) measurements were conducted on aliquots of the same samples at the
130 Center for Ice and Climate (Copenhagen, Denmark) using a Cavity Ring-Down Spectrometer (Picarro, Santa
131 Clara, USA) using the method described by Gkinis et al. (2010). Septum-sealed glass vials were used for these
132 measurements to prevent any sample evaporation during the experimental phases.
133

134

3. Results and discussion

3.1 Stable water isotopes and snow accumulation

The cores were dated based on the seasonal variations identified in the stable water isotopic profiles (both $\delta^{18}O$ and δD). Isotope ratio minima (representing midwinter) can be easily identified (Fig. 2). Almost all of the cores cover the period between 2010 and late 2013, providing four years of snow deposition. The only exception is represented by core 6, whose upper layer is missing.

The annual deposition signal looks less clear in the two cores that were drilled at the sites with the highest elevation and the closest to the Ross Sea, cores TD and 10, and especially for 2013 in core 10. The two sites are probably the most affected by surface remobilization and isotopic diffusion due to low accumulation. Indeed, non-uniformities in the shallow snow layers such as sastrugi, dunes, wind crusts and other features have been identified as an important aspect of the surface morphology around the Talos Dome area (Frezzotti et al., 2004; 2007).

The annual accumulation rates were calculated by selecting the depth intervals included within consecutive maximum or minimum $\delta^{18}O$ values (Table 2) and accounting for the measured density profiles. Table 2 also includes accumulation rates in Victoria Land reported from previous studies. The GV5 site is located between sites 10 and 9 (Fig. 1).

The accumulation rates found during the traverse are in general agreement with the previous works (Becagli et al., 2004; Frezzotti et al., 2007), except for Talos Dome. The accumulation values calculated from the smoothed isotopic profile in Talos Dome are well above those measured by the stake farm (n=41, C. Scarchilli, *personal communication*) for the same years. The fluxes of deposition of sodium, bromine and iodine along the transect are calculated using accumulation rates from this work, except for Talos Dome, where we used the stake farm values.

The accumulation pattern along the transect increases from Talos Dome to the Southern Ocean (GV7, 8, 7, 6), as the previous works have also found (Magand et al., 2004; Frezzotti et al., 2007). Scarchilli et al. (2010) already pointed out how Talos Dome receives 50% of its total precipitation from the north-west (Indian Ocean), 30% from the east (Ross Sea and Pacific Ocean) and approximately 15% from the interior of the plateau. In this picture, our accumulation data show a decrease from the Indian Ocean moving away from the Indian Ocean coasts and approaching Talos Dome.

The sites are located at decreasing altitudes moving from Talos Dome site (highest point) towards the coast facing the Indian sector (site 6). The minimum $\delta^{18}O$ value found in each core shows a decreasing trend with altitude, with an elevation gradient of -1.35 ‰(100m)$^{-1}$. This super-adiabatic lapse rate is confirmed by the surface snow samples collected taken during the 2001/02 ITASE traverse (Magand et al., 2004).

3.2 Sodium, Bromine and Iodine

The main statistical parameters of the measured samples are summarized in Table 3. Sodium shows a mean concentration of 34 ppb, in agreement with published values in this area (Becagli et al., 2004, Bertler et al., 2005, Severi et al., 2009). Among the three elements, sodium shows the highest standard deviation (61%) because of the high variability of sea spray inputs at coastal sites. Singularities up to 200 ppb are probably associated to sea salt rich marine storms. Iodine has an average concentration of 43 ppt, associated with a lower variability compared to bromine and sodium.

The bromine enrichment has been calculated as the bromine excess with respect to sea water concentrations, $Brenr = [Br]/(0.006 \cdot [Na])$, where [Br] and [Na] are the bromine and sodium concentrations in the sample and 0.006 is the bromine-to-sodium concentration ratio in sea water (Millero, 2008). Benassai et al. (2005) have concluded that sea-salt sodium is the dominant fraction (more than 80%) of the total sodium budget in this area. No correction to sodium was therefore applied for this calculation. Despite bromine being a sea salt

The Cryosphere
Discussions

184 marker like sodium, it is recycled over halogen rich sea ice surfaces (i.e. first year sea ice, FYSI) and suspended
185 sea salt aerosol, and exponentially released as Br_2, Eq. (1):

187
$$HOBr + HBr \rightarrow Br_2 + H_2O \qquad\qquad (1)$$
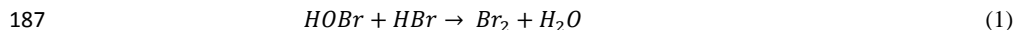
189   Therefore, bromine enrichment signals sea ice presence, on the hypothesis that sodium is left unchanged from
190 emission to deposition. Bromine enrichment has already been linked to sea ice presence in both Arctic and
191 Antarctic coastal sites (Spolaor et al., 2013b, 2014, 2016; Vallelonga et al., 2016).

192 The entire set of bromine enrichment values is visible in Fig. 3. The values extend from a minimum of 0.5 to
193 17, with an average of 4.6 ± 0.1. Notably, more than 98% of the samples show values greater than 1 (i.e. sea
194 water value). A detailed insight on the few <1 values revealed that these samples are associated with very high
195 contributions of sodium inputs (>120 ppb), therefore likely associated to strong marine events. Such
196 distribution of enrichment supports the theory that this parameter is, in these coastal sites, a marker of sea salt
197 aerosol with an extra contribution from sea ice.

198 Figures 4-5-6 and 7 show the variabilities of $\delta^{18}O$ (upper plot), sodium (middle plot, left axis), bromine (middle
199 plot, right axis), iodine (lower plot, right axis) and bromine enrichment (lower plot, left axis) on an age scale
200 for the different coring sites. Thick lines represent 3-month running means of the raw data (circles).

201 Sodium timeseries show great variability: peaks are often found in summer, although they are also observed
202 in winter in cores TD and 8. These findings confirm that, as previous works pointed out (Curran et. al., 1998),
203 in coastal sites storm events carrying open ocean sea salts are more important than sea ice as a sea salt source,
204 although the high level of variability suggests also that meteorology and natural variability play a role. Bromine
205 and bromine enrichment show annual variations, with maximum values in during late spring-summer. Iodine
206 shows a more stable signal throughout the year and high winter singularities in cores TD, GV7 and 8.

207 The timing of the bromine enrichment signal in ice cores relies on the combined effect of sea ice and sunlight,
208 responsible for the photochemical production and release of molecular bromine, Br_2 (Pratt et al., 2013). Sea
209 ice area in the 130-190° E sector was calculated for the 2010-2013 period using web available NSIDC passive
210 microwave sea ice concentration data (Meier et al., 2013). Figures 8 and 9 show the minimum and maximum,
211 found in January 2010 and August 2011, respectively. The monthly sea ice areas from 2010 to 2013 were
212 calculated for such sector and plotted in Fig. 9a (blue); each monthly value was normalized to the total annual
213 sea ice area. The minimum sea ice is found in February, while a longer lasting maximum throughout winter
214 and spring is observed, before a rapid decrease from November. Monthly insolation values were recovered
215 from the Japanese Syowa Station (69° S, 39° E), Fig. 9a (red points).

216 The sub annual distribution of bromine enrichment along the transect is shown in Fig. 9b (blue). Each bins
217 contains the cumulative monthly value for every year in every core, normalized by the total value of each year
218 (which may change according to year and location). The histogram is then normalized by the overall sum
219 measured in the transect. The distribution shows a clear sub-annual oscillation with lowest and highest annual
220 contribution in May (late autumn) and November (late spring), respectively. The combined effect of sea ice
221 and insolation (Fig. 9b, magenta product distribution) shows the same features, with maximum in spring. Such
222 comparison demonstrates the dependency of bromine enrichment on the combined effect of sea ice and
223 insolation. Monthly sea ice area values are reported in Fig. 9c (blue), together with annual averaged values of
224 bromine enrichment (black) and first year sea ice, FYSI (red), calculated as the difference of maximum and
225 minimum sea ice area. A coherent trend in both Br_{enr} and FYSI is observed for the first three years, and not for
226 the last one, although uncertainties cannot exclude a consistency over the whole period. A longer record would
227 be needed to evaluate the correlation and quantitatively reconstruct past sea ice in this sector.

228 Table 4 shows the average annual iodine concentrations for each location, together with its standard deviation.
229 The mean values (0.043 ppb on average) are close to the background values found in Antarctic shallow firn
230 cores near the research stations of Neumayer (Frieß et al., 2010) and Casey (Law Dome, Spolaor et al., 2014)
231 respectively. Unlike previous observations of a clear winter peak of iodine with concentrations up to 0.6 ppb
232 (Neumayer) and 0.3 ppb (Law Dome), no clear seasonality is observed for the transect samples, with annual

233 variability around 10-15%. Core 7 (Fig. 6) shows some variability which corresponds to winter peaks. High
234 iodine concentrations are observed in core 8 during the 2012 winter, in association to a strong sea salt (sodium)
235 input, although similar strong winter peaks are observed in 2011 at GV7 and TD sites.

236 The low background level and low variability of iodine found along the transect reflect a low input of iodine
237 in this area of Antarctica compared to other locations. This picture is confirmed by tropospheric measurements
238 of IO from satellites (Fig. 10, right panel), which show IO concentrations close to detection limit over the area
239 of the transect compared to Law Dome, Neumayer, or any other coastal location. The high elevation of the
240 traverse area, compared to the others is likely to play a role in preventing efficient iodine transport from the
241 source areas.

242 Frieß et al. (2010) and Spolaor et al. (2014) have attributed iodine seasonal signal pattern to summertime
243 photochemical recycling of IO from the snowpack, leading to depletion in the summer layers and higher
244 concentrations in winter when the polar night starts. The lower variability found across the Northern Victoria
245 Land traverse cores could result from a reduced summer recycling due to low iodine concentrations available
246 the snow.

3.3 Spatial flux variability

248 Glaciochemistry around Antarctica is very strongly influenced, among several properties, by the distance from
249 the sea and the pathways of the air mass trajectories (Bertler et al., 2005). Atmospheric circulation patterns
250 around the Talos Dome area have been studied by Scarchilli et al. (2010), who have shown that the main input
251 is represented by the Southern Ocean (Indian sector) with a lower contribution from the Ross Sea.

252 The spatial variability of sodium, bromine and iodine is investigated in Fig. 11. The twelve panels show the
253 mean annual fluxes for each core in relation to the distance from the Indian Ocean. Sodium fluxes show the
254 highest values and variability around the closest locations to the Southern Ocean (GV7, 8, 7, 6), where the
255 accumulation increases. After rapidly decreasing within the first 100 km, the sodium flux becomes stable, as
256 the input from the SO decreases but the one from the Ross sea gradually increases. Talos Dome, the closest
257 location to the Ross sea (290 km from the Indian Ocean – point on the furthest right in every plot of Fig. 11)
258 shows an average annual sodium flux of (2400 ± 970) µg m^{-2} yr^{-1}, consistent, within uncertainties, with the
259 value of (1500 ± 500) µg m^{-2} yr^{-1} found by Spolaor et al. (2013b). Bromine exhibits a similar behavior to
260 sodium, with a homogeneous flux within cores TD, 10 and 9 and an increase (up to 3 times) in the last 100
261 km from the SO. Elevation could partly account for the fractionation of sodium and bromine, having the 180
262 m of height difference separating GV7,8,7 and 6, and 360 m from GV7 to Talos Dome. The effect of
263 elevation yet is combined to the influence of the distance from the source in order to resolve the two effects.
264 A slightly lower fractionation after 100 km from the SO is observed for iodine, confirming the homogeneous
265 satellite measurements of IO (Fig. 10, right).

266

The Cryosphere

Discussions

Open Access

EGU

4. Conclusions

The 2013/14 Talos Dome – GV7 traverse provided an opportunity to expand the existing sodium dataset in Victoria Land and investigate important features of bromine and iodine temporal and spatial variabilities, so far only available in Antarctica at Law Dome and Neumayer station.

The accumulation rates agree with previous studies, with increasing values from the Ross Sea to the Southern Ocean. Accumulation rates calculated for Talos Dome are higher than previously reported, likely caused by isotopic diffusion and remobilization at this site. The locations near the Southern Ocean exhibit high variability due to the higher accumulation.

Sodium and bromine concentrations in the snow samples result in a positive bromine enrichment to seawater, confirming the sea ice influence in the area for the extra bromine deposition. While sodium does not capture clear sub-annual variations associated with sea ice, bromine enrichment shows consistent seasonal variabilities with late spring maxima (November). It is possible to relate such seasonality to the combined effect of sea ice growth and sunlight, which trigger photochemistry above fresh sea ice. The timing of deposition is coherent among Victoria Land, Law Dome (Indian sector) and Neumayer (Atlantic sector). Iodine shows an average value of 0.04 ppb, similar to background values observed in the Antarctic coastal locations of Law Dome and Neumayer. Unlike those locations, low iodine annual variability and no consistent seasonality of the signal are observed in the traverse samples.

The spatial variability study reveals homogeneous fluxes over the transect length, with an increase in absolute values and variability at the sites close to the Indian Ocean, due to high accumulation and proximity to the coasts. Uniform satellite values of BrO and IO over Victoria Land confirm the snow measurements. A fractionation due to distance of these proxies is not found probably due to the combined double input of air masses from the Ross Sea and the Indian Ocean. A transect towards the interior of the plateau would give an insight on this feature.

The trends of annual bromine enrichment and first year sea ice in the 130-190° E sector are comparable, supporting the use of bromine enrichment as FYSI proxy.

Acknowledgements

The Cryosphere
Discussions
Open Access
EGU

References

310

311 (1) Abram, N. J., Curran, M. A. J., Mulvaney, R. and Vance, T.: The preservation of
312   methanesulphonic acid in frozen ice-core samples, J. Glaciol., 54(187), 680–684,
313   doi:10.3189/002214308786570890, 2008.

314

315 (2) Abram, N. J., Thomas, E. R., McConnell, J. R., Mulvaney, R., Bracegirdle, T. J., Sime, L. C.
316   and Aristarain, A. J.: Ice core evidence for a 20th century decline of sea ice in the
317   Bellingshausen Sea, Antarctica, J. Geophys. Res. Atmos., 115(23), 1–9,
318   doi:10.1029/2010JD014644, 2010.

319

320 (3) Abram, N. J., Wolff, E. W. and Curran, M. A. J.: A review of sea ice proxy information from
321   polar ice cores, Quat. Sci. Rev., 79, 168–183, doi:10.1016/j.quascirev.2013.01.011, 2013.

322

323 (4) Adams, J. W., Holmes, N. S. and Crowley, J. N.: Uptake and reaction of HOBr on frozen and
324   dry NaCl/NaBr surfaces between 253 and 233 K, Atmos. Chem. Phys., 2, 79–91,
325   doi:10.5194/acp-2-79-2002, 2002.

326

327 (5) Albani, S., Delmonte, B., Maggi, V., Baroni, C., Petit, J. R., Stenni, B., Mazzola, C. and
328   Frezzotti, M.: Interpreting last glacial to Holocene dust changes at Talos Dome (East
329   Antarctica): Implications for atmospheric variations from regional to hemispheric scales,
330   Clim. Past, 8(2), 741–750, doi:10.5194/cp-8-741-2012, 2012.

331

332 (6) Atkinson, H. M., Huang, R. J., Chance, R., Roscoe, H. K., Hughes, C., Davison, B.,
333   Schönhardt, A., Mahajan, A. S., Saiz-Lopez, A., Hoffmann, T. and Liss, P. S.: Iodine
334   emissions from the sea ice of the Weddell Sea, Atmos. Chem. Phys., 12(22), 11229–11244,
335   doi:10.5194/acp-12-11229-2012, 2012.

336

337 (7) Baccolo, G., Clemenza, M., Delmonte, B., Maffezzoli, N., Nastasi, M., Previtali, E., Prata,
338   M., Salvini, A. and Maggi, V.: A new method based on low background instrumental neutron
339   activation analysis for major, trace and ultra-trace element determination in atmospheric
340   mineral dust from polar ice cores, Anal. Chim. Acta, 1–8, doi:10.1016/j.aca.2016.04.008,
341   2016.

342

The Cryosphere

Open Access

EGU

Discussions

343   (8) Barrie, L. a., Bottenheim, J. W., Schnell, R. C., Crutzen, P. J. and Rasmussen, R. a.: Ozone
344   destruction and photochemical reactions at polar sunrise in the lower Arctic atmosphere,
345   Nature, 334(6178), 138–141, doi:10.1038/334138a0, 1988.

346

347   (9) Becagli, S., Benassai, S., Castellano, E., Largiuni, O., Migliori, A., Traversi, R., Flora, O. and
348   Udisti, R.: Chemical characterization of the last 250 years of snow deposition at Talos Dome
349   (East   Antarctica),   Int.   J.   Environ.   Anal.   Chem.,   84(6-7),   523–536,
350   doi:10.1080/03067310310001640384, 2004.

351

352   (10)   Becagli, S., Proposito, M., Benassai, S., Flora, O., Genoni, L., Gragnani, R., Largiuni,
353   O., Pili, S. L., Severi, M., Stenni, B., Traversi, R., Udisti, R. and Frezzotti, M.: Chemical and
354   isotopic snow variability in East Antarctica along the 2001/02 ITASE traverse, Ann. Glaciol.,
355   39, 473–482, doi:10.3189/172756404781814636, 2004.

356

357   (11)   Becagli, S., Proposito, M., Benassai, S., Gragnani, R., Magand, O., Traversi, R. and
358   Udisti, R.: Spatial distribution of biogenic sulphur compounds (MSA, $nssSO_4^{2-}$) in the
359   northern Victoria Land – Dome C – Wilkes Land area , East Antarctica, Ann. Glaciol., 23–
360   31, doi:10.3189/172756405781813384, 2005.

361

362   (12)   Bertler, N., Mayewski, P. A., Aristarain, A., Barrett, P., Becagli, S., Bernardo, R., Bo,
363   S., Xiao, C., Curran, M., Qin, D., Dixon, D. A., Ferron, F., Fischer, H., Frey, M., Frezzotti,
364   M., Fundel, F., Genthon, C., Gragnani, R., Hamilton, G. S., Handley, M., Hong, S., Isaksson,
365   E., Kang, J., Ren, J., Kamiyama, K., Kanamori, S., Kärkäs, E., Karlöf, L., Kaspari, S., Kreutz,
366   K., Kurbatov, A., Meyerson, E., Ming, Y., Zhang, M., Motoyama, H., Mulvaney, R., Oerter,
367   H., Osterberg, E., Proposito, M., Pyne, A., Ruth, U., Simões, J., Smith, B., Sneed, S., Teinilä,
368   K., Traufetter, F., Udisti, R., Virkkula, A., Watanabe, O., Williamson, B., Winther, J. G., Li,
369   Y., Wolff, E., Li, Z. and Zielinski, A.: Snow chemistry across Antarctica, Ann. Glaciol., 41,
370   167–179, doi:10.3189/172756405781813320, 2005.

371
372

373   (13)   Curran, M. A. J., Van Ommen, T. D., Morgan, Vin: Seasonal characteristics of the
374   major ions in the high-accumulation Dome Summit South ice core, Law Dome, Antarctica,
375   Ann. Glaciol., 27(1998), 385-390(6), doi:10.3198/1998AoG27-1-385-390, 1998.

376

377   (14)   Curran, M. A. J., van Ommen, T. D., Morgan, V. I., Phillips, K. L. and Palmer, A. S.:
378   Ice Core Evidence for Antarctic Sea Ice Decline Since the1950s, Science (80-.)., 302(5648),
379   1203–1206, doi:10.1126/science.1087888, 2003.

380

The Cryosphere
Discussions
Open Access
EGU

381 (15)   Delmas, B. R. J., Wagnon, P., Kamiyama, K. and Watanabe, O.: Evidence for the loss
382   of snow-deposited MSA to the interstitial gaseous phase in central Antarctic firn, Tellus B,
383   55(1), 71–79, doi:10.1034/j.1600-0889.2003.00032.x, 2003.

384

385 (16)   Delmonte, B., Baroni, C., Andersson, P. S., Schoberg, H., Hansson, M., Aciego, S.,
386   Petit, J. R., Albani, S., Mazzola, C., Maggi, V. and Frezzotti, M.: Aeolian dust in the Talos
387   Dome ice core (East Antarctica, Pacific/Ross Sea sector): Victoria Land versus remote sources
388   over the last two climate cycles, J. Quat. Sci., 25(8), 1327–1337, doi:10.1002/jqs.1418, 2010.

389

390 (17)   Delmonte, B., Andersson, P. S., Schöberg, H., Hansson, M., Petit, J. R., Delmas, R.,
391   Gaiero, D. M., Maggi, V. and Frezzotti, M.: Geographic provenance of aeolian dust in East
392   Antarctica during Pleistocene glaciations: preliminary results from Talos Dome and
393   comparison with East Antarctic and new Andean ice core data, Quat. Sci. Rev., 29(1-2), 256–
394   264, doi:10.1016/j.quascirev.2009.05.010, 2010.

395

396 (18)   Delmonte, B., Baroni, C., Andersson, P. S., Narcisi, B., Salvatore, M. C., Petit, J. R.,
397   Scarchilli, C., Frezzotti, M., Albani, S. and Maggi, V.: Modern and Holocene aeolian dust
398   variability from Talos Dome (Northern Victoria Land) to the interior of the Antarctic ice sheet,
399   Quat. Sci. Rev., 64, 76–89, doi:10.1016/j.quascirev.2012.11.033, 2013.

400

401 (19)   Frezzotti, M., Bitelli, G., De Michelis, P., Deponti, A., Forieri, A., Gandolfi, S., Maggi,
402   V., Mancini, F., Remy, F., Tabacco, I. E., Urbini, S., Vittuari, L. and Zirizzottl, A.:
403   Geophysical survey at Talos Dome, East Antarctica: The search for a new deep-drilling site,
404   Ann. Glaciol., 39(2002), 423–432, doi:10.3189/172756404781814591, 2004.

405

406 (20)   Frezzotti, M., Urbini, S., Proposito, M., Scarchilli, C. and Gandolfi, S.: Spatial and
407   temporal variability of surface mass balance near Talos Dome, East Antarctica, J. Geophys.
408   Res. Earth Surf., 112(2), doi:10.1029/2006JF000638, 2007.

409

410 (21)   Frieß, U., Deutschmann, T., Gilfedder, B. S., Weller, R. and Platt, U.: Iodine monoxide
411   in the Antarctic snowpack, Atmos. Chem. Phys., 10(5), 2439–2456, doi:10.5194/acp-10-
412   2439-2010, 2010.

413

414 (22)   Gkinis, V., Popp, T. J., Johnsen, S. J. and Blunier, T.: A continuous stream flash
415   evaporator for the calibration of an IR cavity ring-down spectrometer for the isotopic analysis
416   of   water.,   Isotopes   Environ.   Health   Stud.,   46(11),   463–475,
417   doi:10.1080/10256016.2010.538052, 2010.

The Cryosphere
Discussions

Open Access

EGU

418

419   (23)   Grootes, P. M., Steig, E. J., Stuiver, M., Waddington, E. D., Morse, D. L. and Nadeau,
420   M.-J.: The Taylor Dome Antarctic 18O Record and Globally Synchronous Changes in
421   Climate, Quat. Res., 56(3), 289–298, doi:10.1006/qres.2001.2276, 2001.

422

423   (24)   Isaksson, E., Kekonen, T., Moore, J. and Mulvaney, R.: The methanesulfonic acid
424   (MSA)   record   in   a   Svalbard   ice   core,   Ann.   Glaciol.,   42(9296),   345–351,
425   doi:10.3189/172756405781812637, 2005.

426

427   (25)   Magand, O., Frezzotti, M., Pourchet, M., Stenni, B., Genoni, L. and Fily, M.: Climate
428   variability along latitudinal and longitudinal transects in East Antarctica, Ann. Glaciol., 39,
429   351–358, doi:10.3189/172756404781813961, 2004.

430

431   (26)   Mahajan, A. S., Shaw, M., Oetjen, H., Hornsby, K. E., Carpenter, L. J., Kaleschke, L.,
432   Tian-Kunze, X., Lee, J. D., Moller, S. J., Edwards, P., Commane, R., Ingham, T., Heard, D.
433   E. and Plane, J. M. C.: Evidence of reactive iodine chemistry in the Arctic boundary layer, J.
434   Geophys. Res. Atmos., 115(20), 1–11, doi:10.1029/2009JD013665, 2010.

435
436

437   (27)   Mayewski, P.A., Frezzotti, M., Bertler, N., Van Ommen T., Hamilton, G., Jacka, T.
438   H., Welch, B., Frey, M., Dahe, Q., Jiawen, R., Simöes, J., Fily, M., Oerter, H., Nishio,
439   F., Isaksson, E., Mulvaney, R., Holmund, P., Lipenkov, V. and Goodwin, I.: The International
440   Trans-Antarctic Scientific Expedition (ITASE): An overview, Ann. Glaciol., 41, 180–185,
441   doi:10.3189/172756405781813159, 2005.

442

443   (28)   Meier, W., F. Fetterer, M. Savoie, S. Mallory, R. Duerr, and J. Stroeve: NOAA/NSIDC
444   Climate Data Record of Passive Microwave Sea Ice Concentration, Version 2, Boulder,
445   Colorado USA. NSIDC: National Snow and Ice Data Center. [September 05, 2016]. Doi:
446   http://dx.doi.org/10.7265/N55M63M1, 2013, updated 2015.

447   (29)   Millero, F. J., Feistel, R., Wright, D. G. and McDougall, T. J.: The composition of
448   Standard Seawater and the definition of the Reference-Composition Salinity Scale, Deep Sea
449   Res. Part I Oceanogr. Res. Pap., 55(1), 50–72, doi:10.1016/j.dsr.2007.10.001, 2008.

450

451   (30)   Pratt, K. a., Custard, K. D., Shepson, P. B., Douglas, T. a., Pöhler, D., General, S.,
452   Zielcke, J., Simpson, W. R., Platt, U., Tanner, D. J., Gregory Huey, L., Carlsen, M. and Stirm,
453   B. H.: Photochemical production of molecular bromine in Arctic surface snowpacks, Nat.
454   Geosci., 6(5), 351–356, doi:10.1038/ngeo1779, 2013.

The Cryosphere

Discussions

Open Access

EGU

455

(31)   Proposito, M., Becagli, S., Castellano, E., Flora, O., Genoni, L., Gragnani, R., Stenni, B., Traversi, R., Udisti, R. and Frezzotti, M.: Chemical and isotopic snow variability along the 1998 ITASE traverse from Terra Nova Bay to Dome C, East Antarctica, Ann. Glaciol., 35, 187–194, doi:10.3189/172756402781817167, 2002.

460

(32)   Röthlisberger, R. and Abram, N.: Sea-ice proxies in Antarctic ice cores, PAGES News, 17(1), 24–26, 2009.

463

(33)   Saiz-Lopez, A., Mahajan, A. S., Salmon, R. A., Bauguitte, S. J.-B., Jones, A. E., Roscoe, H. K. and Plane, J. M. C.: Boundary Layer Halogens in Coastal Antarctica, Science (80-.)., 317(5836), 348–351, doi:10.1126/science.1141408, 2007.

467

(34)   Saiz-Lopez, A. and von Glasow, R.: Reactive halogen chemistry in the troposphere, Chem. Soc. Rev., 41(19), 6448, doi:10.1039/c2cs35208g, 2012.

470

(35)   Sala, M., Delmonte, B., Frezzotti, M., Proposito, M., Scarchilli, C., Maggi, V., Artioli, G., Dapiaggi, M., Marino, F., Ricci, P. C. and De Giudici, G.: Evidence of calcium carbonates in coastal (Talos Dome and Ross Sea area) East Antarctica snow and firn: Environmental and climatic implications, Earth Planet. Sci. Lett., 271(1-4), 43–52, doi:10.1016/j.epsl.2008.03.045, 2008.

476

(36)   Scarchilli, C., Frezzotti, M. and Ruti, P. M.: Snow precipitation at four ice core sites in East Antarctica: Provenance, seasonality and blocking factors, Clim. Dyn., 37(9-10), 2107–2125, doi:10.1007/s00382-010-0946-4, 2011.

480

(37)   Schönhardt, A., Richter, A., Wittrock, F., Kirk, H., Oetjen, H., Roscoe, H. K. and Burrows, J. P.: Observations of iodine monoxide columns from satellite, Atmos. Chem. Phys., 8(3), 637–653, doi:10.5194/acp-8-637-2008, 2008.

484

(38)   Schönhardt, A., Begoin, M., Richter, A., Wittrock, F., Kaleschke, L., Gómez Martín, J. C. and Burrows, J. P.: Simultaneous satellite observations of IO and BrO over Antarctica, Atmos. Chem. Phys., 12(14), 6565–6580, doi:10.5194/acp-12-6565-2012, 2012.

488

The Cryosphere
Discussions

Open Access

EGU

489   (39)   Schüpbach, S., Federer, U., Kaufmann, P. R., Albani, S., Barbante, C., Stocker, T. F.
490   and Fischer, H.: High-resolution mineral dust and sea ice proxy records from the Talos Dome
491   ice core, Clim. Past, 9(6), 2789–2807, doi:10.5194/cp-9-2789-2013, 2013.

492

493   (40)   Severi, M., Becagli, S., Castellano, E., Morganti, A., Traversi, R. and Udisti, R.: Thirty
494   years of snow deposition at Talos Dome (Northern Victoria Land, East Antarctica): Chemical
495   profiles   and   climatic   implications,   Microchem.   J.,   92(1),   15–20,
496   doi:10.1016/j.microc.2008.08.004, 2009.

497

498   (41)   Spolaor, A., Gabrieli, J., Martma, T., Kohler, J., Björkman, M. B., Isaksson, E., Varin,
499   C., Vallelonga, P., Plane, J. M. C. and Barbante, C.: Sea ice dynamics influence halogen
500   deposition to Svalbard, Cryosph., 7(5), 1645–1658, doi:10.5194/tc-7-1645-2013, 2013a.
501
502
503   (42)   Spolaor, A., Vallelonga, P., Plane, J. M. C., Kehrwald, N., Gabrieli, J., Varin, C.,
504   Turetta, C., Cozzi, G., Kumar, R., Boutron, C. and Barbante, C.: Halogen species record
505   Antarctic sea ice extent over glacial-interglacial periods, Atmos. Chem. Phys., 13(13), 6623–
506   6635, doi:10.5194/acp-13-6623-2013, 2013b.
507
508
509   (43)   Spolaor, A., Vallelonga, P., Gabrieli, J., Martma, T., Björkman, M. P., Isaksson, E.,
510   Cozzi, G., Turetta, C., Kjær, H. A., Curran, M. A. J., Moy, A. D., Schönhardt, A.,
511   Blechschmidt, A. M., Burrows, J. P., Plane, J. M. C. and Barbante, C.: Seasonality of halogen
512   deposition in polar snow and ice, Atmos. Chem. Phys., 14(18), 9613–9622, doi:10.5194/acp-
513   14-9613-2014, 2014.
514
515   (44)   Spolaor, A., Opel, T., McConnell, J. R., Maselli, O. J., Spreen, G., Varin, C.,
516   Kirchgeorg, T., Fritzsche, D. and Vallelonga, P.: Halogen-based reconstruction of Russian
517   Arctic sea ice area from the Akademii Nauk ice core (Severnaya Zemlya), Cryosph., 10, 245–
518   256, doi:10.5194/tc-10-245-2016, 2016.
519
520   (45)   Spolaor, A., Vallelonga, P., Turetta, C., Maffezzoli, N., Cozzi, G., Gabrieli, J.,
521   Barbante, C., Goto-Azuma, K., Saiz-Lopez, A., Cuevas, C. A. and Dahl-Jensen, D.: Canadian
522   Arctic sea ice reconstructed from bromine in the Greenland NEEM ice core, Sci. Rep., 6,
523   doi:10.1038/srep33925, 2016.
524
525
526   (46)   Stenni, B., Proposito, M., Gragnani, R., Flora, O., Jouzel, J., Falourd, S. and Frezzotti,
527   M.: Eight centuries of volcanic signal and climate change at Talos Dome (East Antarctica), J.
528   Geophys. Res. Atmos., 107(D9), doi:10.1029/2000JD000317, 2002.
529
530   (47)   Stenni, B., Buiron, D., Frezzotti, M., Albani, S., Barbante, C., Bard, E., Barnola, J. M.,
531   Baroni, M., Baumgartner, M., Bonazza, M., Capron, E., Castellano, E., Chappellaz, J.,
532   Delmonte, B., Falourd, S., Genoni, L., Iacumin, P., Jouzel, J., Kipfstuhl, S., Landais, a.,
533   Lemieux-Dudon, B., Maggi, V., Masson-Delmotte, V., Mazzola, C., Minster, B., Montagnat,
534   M., Mulvaney, R., Narcisi, B., Oerter, H., Parrenin, F., Petit, J. R., Ritz, C., Scarchilli, C.,
535   Schilt, a., Schüpbach, S., Schwander, J., Selmo, E., Severi, M., Stocker, T. F. and Udisti, R.:

The Cryosphere
Discussions
Open Access
EGU

536   Expression of the bipolar see-saw in Antarctic climate records during the last deglaciation,
537   Nat. Geosci., 3(12), 1–4, doi:10.1038/ngeo1026, 2011.
538
539   (48)   Vallelonga, P., Barbante, C., Cozzi, G., Gabrieli, J., Schüpbach, S., Spolaor, A. and
540   Turetta, C.: Iron fluxes to Talos Dome, Antarctica, over the past 200 kyr, Clim. Past, 9(2),
541   597–604, doi:10.5194/cp-9-597-2013, 2013.
542
543   (49)   Vallelonga, P., Maffezzoli, N., Moy, A. D., Curran, M. A. J., Vance, T. R., Edwards,
544   R., Hughes, G., Barker, E., Spreen, G., Saiz-Lopez, A., Corella, J. P., Cuevas, C. A. and
545   Spolaor, A.: Sea ice-related halogen enrichment at Law Dome, coastal East Antarctica, Clim.
546   Past Discuss., (July), 1–26, doi:10.5194/cp-2016-74, 2016.
547
548   (50)   Vogt, R., Crutzen, P. J. and Sander, R.: A mechanism for halogen release from sea-
549   salt aerosol in the remote marine boundary layer, Nature, 383(6598), 327–330,
550   doi:10.1038/383327a0, 1996.
551
552   (51)   Vogt, R., Sander, R., Von Glasow, R. and Crutzen, P. J.: Iodine chemistry and its role
553   in halogen activation and ozone loss in the marine boundary layer: A model study, J. Atmos.
554   Chem., 32(3), 375–395, doi:10.1023/A:1006179901037, 1999.
555
556   (52)   Weller, R., Traufetter, F., Fischer, H., Oerter, H., Piel, C. and Miller, H.:
557   Postdepositional losses of methane sulfonate, nitrate , and chloride at the European Project
558   for Ice Coring in Antarctica deep-drilling site in Dronning Maud Land , Antarctica, , 109(x),
559   1–9, doi:10.1029/2003JD004189, 2004.
560
561   (53)   Wolff, E. W., Fischer, H., Fundel, F., Ruth, U., Twarloh, B., Littot, G. C., Mulvaney,
562   R., Röthlisberger, R., de Angelis, M., Boutron, C. F., Hansson, M., Jonsell, U., Hutterli, M.
563   a, Lambert, F., Kaufmann, P., Stauffer, B., Stocker, T. F., Steffensen, J. P., Bigler, M.,
564   Siggaard-Andersen, M. L., Udisti, R., Becagli, S., Castellano, E., Severi, M., Wagenbach, D.,
565   Barbante, C., Gabrielli, P. and Gaspari, V.: Southern Ocean sea-ice extent, productivity and
566   iron flux over the past eight glacial cycles., Nature, 440(7083), 491–496,
567   doi:10.1038/nature06271, 2006.
568
569

The Cryosphere
Open Access
Discussions
EGU

570   **Table 1.** Core drilling site information.

Core Site	Core depth (cm)	Lat. (S)	Long. (E)	Elevation (m a.s.l)	Distance from Ross sea (km)	Distance from Indian Ocean (km)
TD	200	72° 48'	159° 06'	2315	250	290
10	200	72° 12'	158°41'	2200	310	240
9	200	71° 21'	158° 23'	2151	380	180
GV7	250	70° 41'	158° 51'	1957	430	95
8	200	70° 36'	158° 35'	1934	440	90
7	200	70° 31'	158° 25'	1894	460	90
6	200	70° 21'	158° 24'	1781	470	85

571

572 **Table 2.** Summary of accumulation rate data from Northern Victoria Land. All uncertainties (shown in parentheses) are 1σ errors.
573 (a) this work.
574 * Uncertain due to smoothed isotopic signal.
575 (b) Becagli et al., 2004.
576 (c) Frezzotti et al., 2007.
577 (d) from stake farm (n=41) (C. Scarchilli, *personal communication*).
578 (e) 1966-96 (Stenni et al., 2002).

Core	Accumulation rates (kg m^{-2} yr^{-1})					2001/02 [b]	1965-2001 [c]	2001-2012 [d]
	2013 traverse [a]							
	2013	2012	2011	2010	Average			
TD	223*	144*	187*	-	185 (31)	104 (37)	86.6[e]	71 (4)
	-	66[d]	107[d]	78[d]	81 (17)[d]			
10	260*	140	140	120	133 (9)	GV5 156 (27)	GV5 129 (6)	
9	180	180	180	180	180 (0)			
GV7	228	261	260	156	232 (32)	261 (50)	241 (12)	
8	240	260	280	-	260 (16)			
7	220	180	200	180	195 (18)			
6	-	200	260	200	220 (29)			

579

The Cryosphere

Discussions

Open Access

EGU

580 **Table 3.** Mean parameters for the 2013/14 Talos Dome – GV7 traverse samples. DL = detection limit, calculated as 3 times the
581 standard deviation of the blanks.

	Na (ppb)	I (ppb)	Br (ppb)
# values	373	374	377
Min	9	0.03	0.2
Max	196	0.09	2.2
Mean	34	0.043	0.7
DL	0.8	0.005	0.05
Std dev %	61	23	42

582

The Cryosphere

Discussions

EGU

Open Access

583   **Table 4**. Iodine average concentrations and variability during the 2013-2010 time period. All values are expressed in ppb.

Core	2013		2012		2011		2010	
	I	St. dev.	I	St. dev.	I	St. dev.	I	St. dev.
TD	0.047	0.004	0.044	0.002	0.048	0.013	-	-
10	0.041	0.005	0.043	0.001	0.049	0.008	0.040	0.005
9	0.038	0.003	0.041	0.010	0.046	0.008	0.047	0.003
GV7	0.044	0.004	0.042	0.004	0.043	0.004	0.047	0.005
8	0.033	0.002	0.049	0.021	0.032	0.002	-	-
7	0.038	0.006	0.034	0.004	0.037	0.009	0.041	0.008
6	-	-	0.039	0.002	0.044	0.006	0.041	0.008

584

Figure 1. (a) Schematic map of the traverse area and coring sites, marked with stars. The cores were drilled between Nov 20th 2013 and Jan 8th 2014 (early austral summer). (b) Minimum (left, February) and maximum (right, July) sea ice concentrations in 2010 (NSIDC data from Meier et al., 2013).

The Cryosphere
Discussions

Open Access

EGU
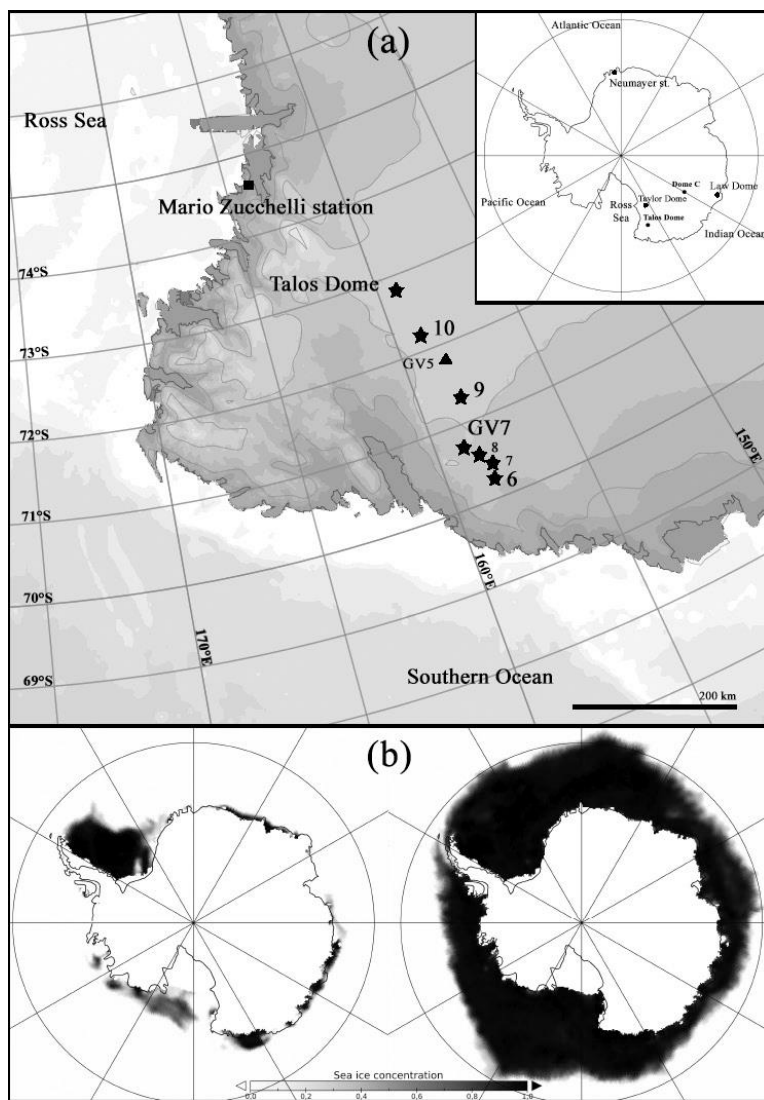
Figure 2. δ¹⁸O (thick line) and δD (dashed line) profiles of the cores. Resolution of sampling is 5 cm. The winter of each year is indicated with lines in correspondence with the water isotope minima. Core 10: the 2013 winter layer is uncertain.

591

The Cryosphere

Open Access

Discussions

EGU
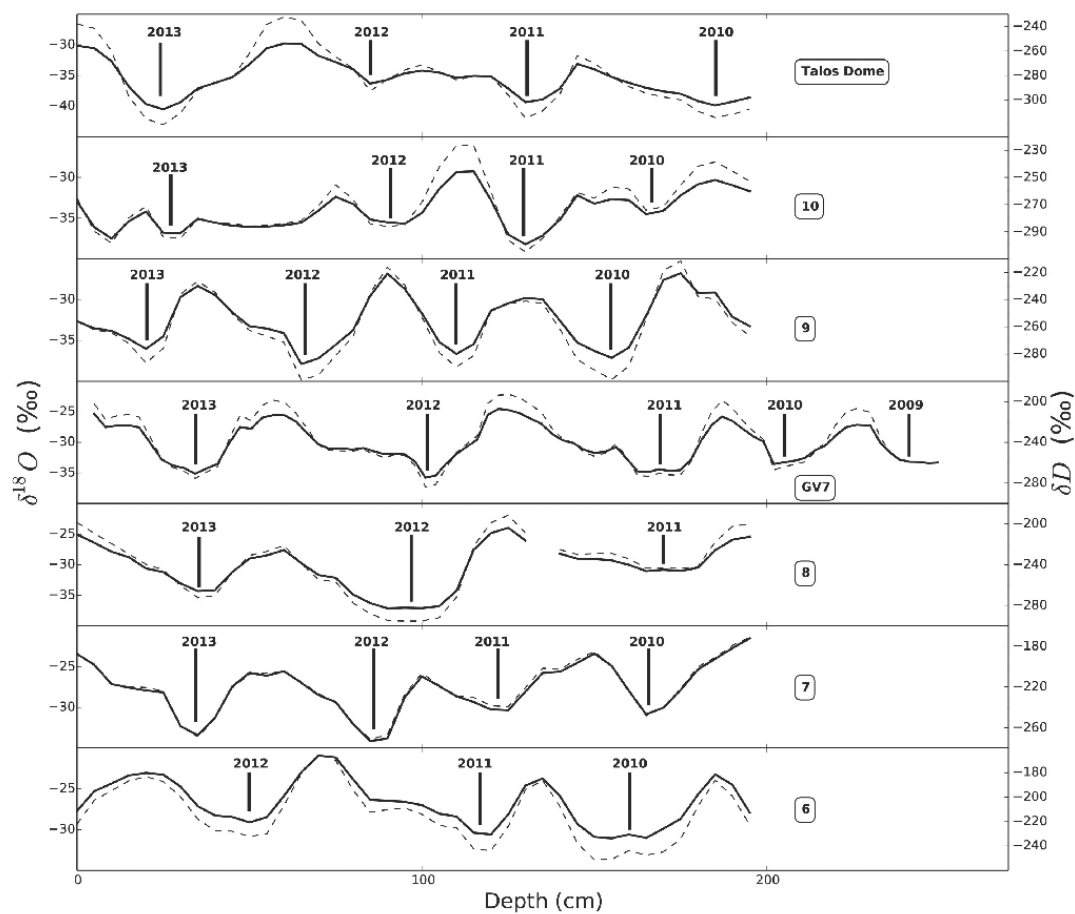
592 **Figure 3**. Distribution of bromine enrichment values of the entire set of samples. The dashed line indicates the seawater value (Br_{enr}
593 $= 1$).
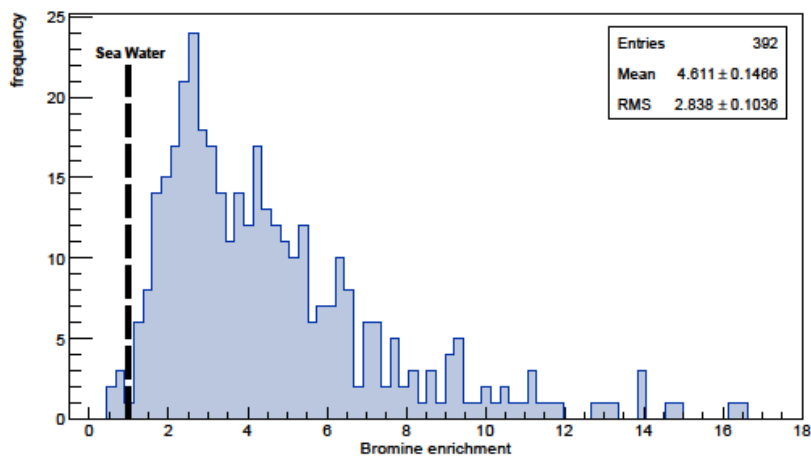
594

595   **Figure 4.** $\delta^{18}O$, Na, Br, Br_{enr} and I profiles in cores TD (left) and 10 (right).
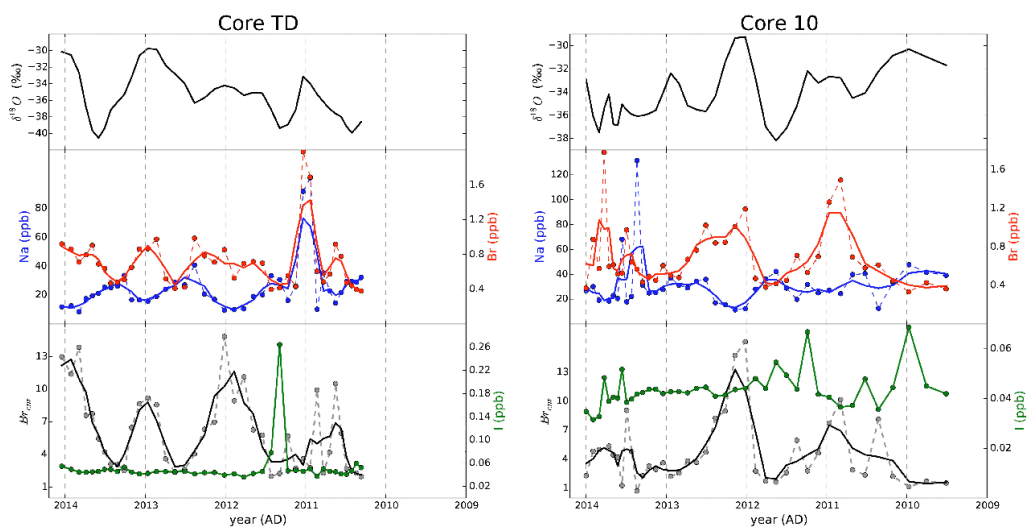
596

597   **Figure 5.** $\delta^{18}O$, Na, Br, Br_{enr} and I profiles in cores 9 (left) and GV7 (right).
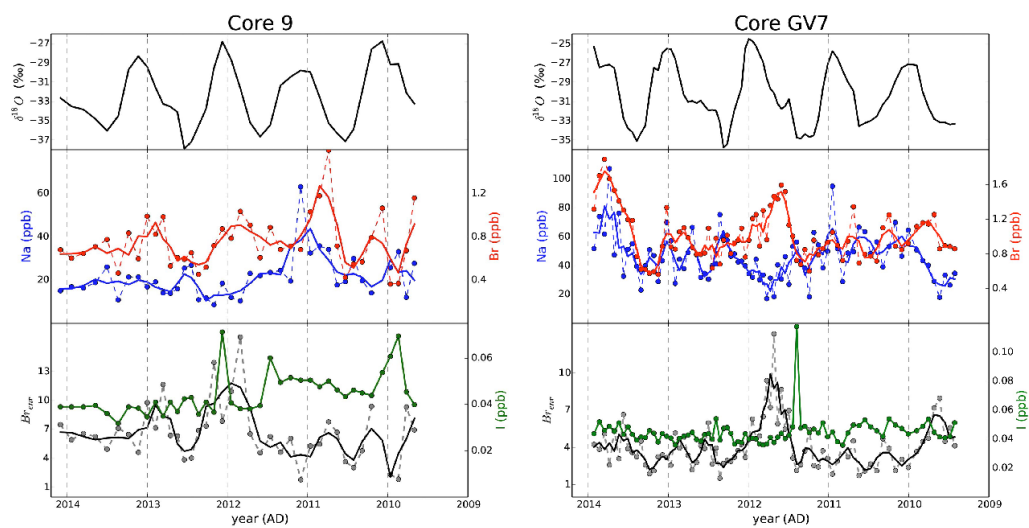
598

599   **Figure 6.** $\delta^{18}O$, Na, Br, Br_{enr} and I profiles in cores 8 (left) and 7 (right).
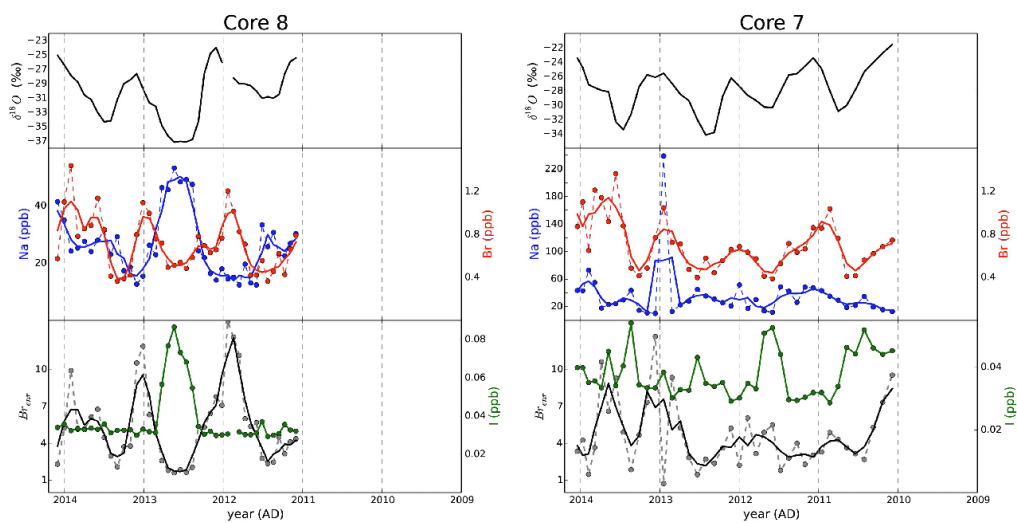
600

601 **Figure 7.** $\delta^{18}O$, Na, Br, Br_{enr} and I profiles in core 6.
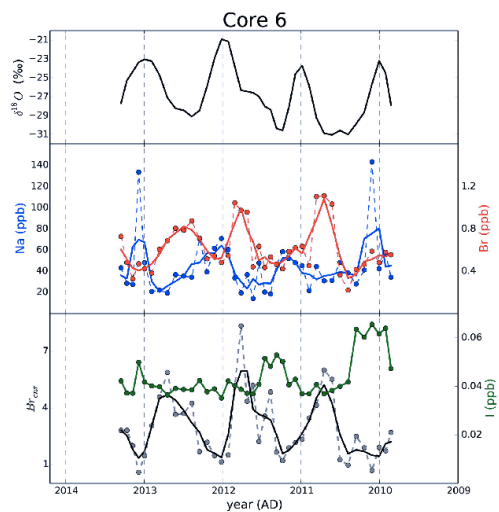
602

603   **Figure 8.** Minimum (a) and maximum (b) sea ice in the 2010-2013 period within 130-190° E longitude sector.


604

605
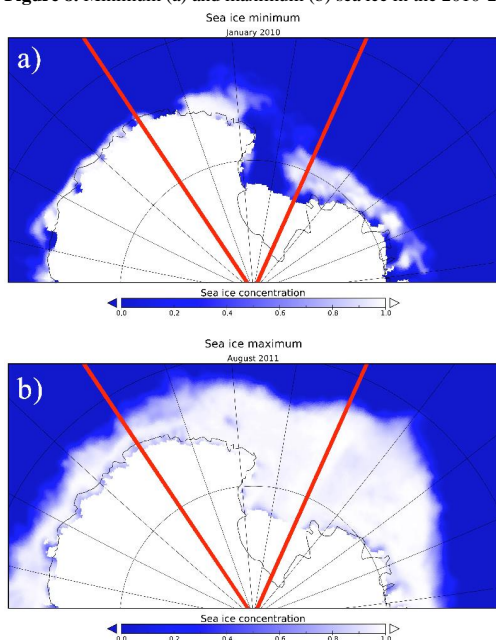
Figure 9. (a) Monthly values of sea ice area (blue) within the 130-190° E sector and solar radiation at 69° S (red).
(b) % of annual bromine enrichment along the traverse, normalized to the total annual amount: the monthly trend shows a seasonal
feature with maximum in late Spring (November). The histogram considers every year and every core of the transect. The shaded blue
area shows the systematic uncertainty associated to the dating. The error bars represent the normalized rms. The magenta band
represents the product distribution of normalized sea ice area and insolation, expressed in annual percentage. **(c)** Monthly sea ice area
values (blue) from 2010 to 2013, with annual values of FYSI (red) and averaged bromine enrichment (black).
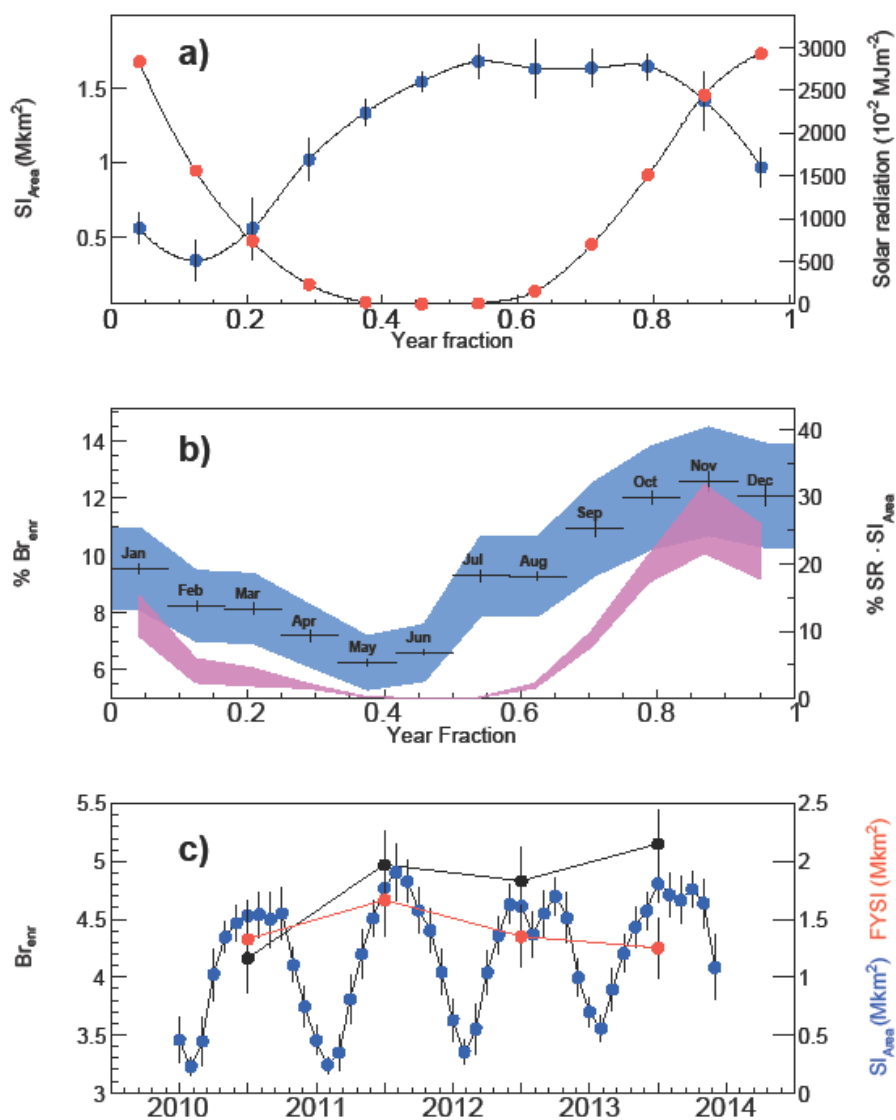
Figure 10. Average atmospheric column concentrations of BrO and IO in Antarctica between 2009 and 2011, from Spolaor et al., 2014.

The Cryosphere
Discussions
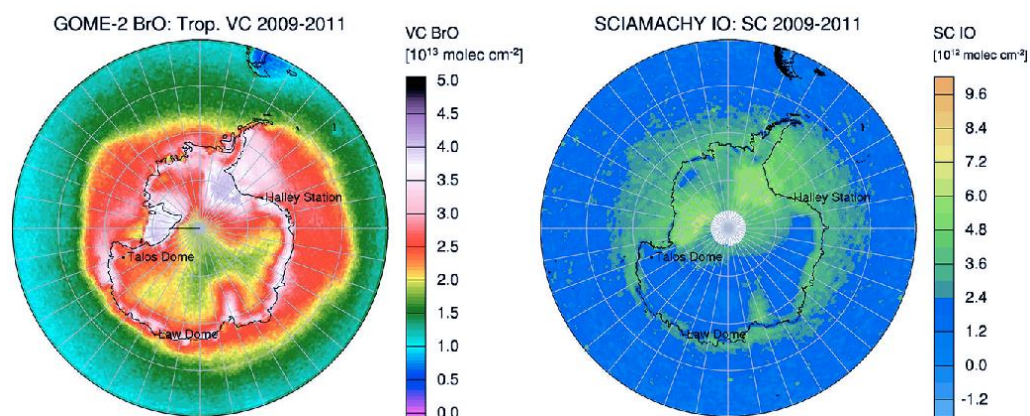
Figure 11. Mean annual fluxes of sodium (blue), bromine (red) and iodine (green) as a function of distance from the Indian Ocean. Each dot represents a location along the traverse.